arXiv:1506.01944v2 [cond-mat.mes-hall] 8 Apr 2016

Unconventional dc transport in Rashba electron gases

Valentina Brosco,[1] Lara Benfatto,[1] Emmanuele Cappelluti,[1] and Claudio Grimaldi[2]

[1] *ISC-CNR and Department of Physics, Sapienza University of Rome, P.le A. Moro 2, 00185 Rome, Italy*
[2] *Laboratory of Physics of Complex Matter, Ecole Polytechnique Fédérale de Lausanne, Station 3, CH-1015 Lausanne, Switzerland*

We discuss the transport properties of a disordered two-dimensional electron gas with strong Rashba spin-orbit coupling. We show that in the high-density regime where the Fermi energy overcomes the energy associated with spin-orbit coupling, dc transport is accurately described by a standard Drude's law, due to a non-trivial compensation between the suppression of back-scattering and the relativistic correction to the quasi-particle velocity. On the contrary, when the system enters the opposite *dominant* spin-orbit regime, Drude's paradigm breaks down and the dc conductivity becomes strongly sensitive to the spin-orbit coupling strength, providing a suitable tool to test the entanglement between spin and charge degrees of freedom in these systems.

PACS numbers: 71.70.Ej, 72.15.-v

Spin-orbit (SO) coupling is a fundamental ingredient in spintronics[1] as it provides an advantageous locking between spin and electron orbital momentum. Recently, intense research efforts [2] have been devoted to two-dimensional (2D) materials with broken inversion symmetry, where the SO strength, parametrized by a characteristic energy scale, E_0, can be tuned by means of external conditions (electric fields, gating, doping, pressure, strain, ...). In most of these systems (ex.: surface alloys [3–9], layered bismuth tellurohalides [10–16], HgTe quantum wells [17], interfaces between complex oxides [18–32]) the total charge carrier density n can be tuned down to very small concentrations, implying very small Fermi energies $E_{\rm F}$. Although the high-density (HD) regime $E_{\rm F} \gtrsim E_0$ has been widely investigated[2, 33–38], relatively less attention has been paid to the opposite regime of dominant SO (DSO), $E_0 \gtrsim E_{\rm F}$.

In this Letter we provide a detailed investigation of the dc conductivity of a 2D electron gas (2DEG) with Rashba[39] SO coupling in the different density regimes. Using a Boltzmann approach and a fully quantum analysis based on Kubo formula, we show that in the high-density regime $E_{\rm F} \gtrsim E_0$, dc transport is *independent* of the SO strength, and the dc conductivity σ_{dc} of electrons having effective mass m and scattering time τ_0 follows the conventional Drude law for 2DEGs,

$$\sigma_{\rm Drude} = \frac{ne^2\tau_0}{m}, \tag{1}$$

that results from a *non-trivial* cancellation of the SO coupling effects on the quasiparticle velocity and transport scattering time. Remarkably, as soon as the system enters the DSO regime $E_0 \gtrsim E_{\rm F}$, Drude's paradigm (1) breaks down and the dc conductivity accurately follows the analytical formula:

$$\sigma_{\rm DSO} = \frac{e^2\tau_0 n_0}{2\,m}\left(\frac{n^4}{n_0^4}+\frac{n^2}{n_0^2}\right) \quad n \le n_0, \tag{2}$$

where $n_0 = 2mE_0/(\pi\hbar^2)$ is the density at $E_F = E_0$. In contrast to the linear dependence of σ_{dc} on the charge density found in the HD regime, $n \ge n_0$, Eq. (2) predicts an *unconventional* non-linear behavior of σ_{dc} with n, that is controlled by the SO interaction encoded in n_0. The relevance of this result is twofold: demonstrating that dc transport is strongly sensitive to Rashba SO coupling, not only it suggests that SO coupling could be measured in a transport experiment but also, what is more important for applications, it points at the possibility of tuning the conductivity of a 2DEG by tuning the SO coupling strength *via* external gates.

A disordered Rashba 2DEG confined to the (x, y)-plane is described by the following Hamiltonian

$$H = \int d\mathbf{r}\, \Psi^\dagger(\mathbf{r})\left[\frac{p^2}{2m} + \alpha\, \hat{z}\cdot(\mathbf{p}\times\vec{\sigma}) + V_{\rm imp}(\mathbf{r})\right]\Psi(\mathbf{r}), \tag{3}$$

where $V_{\rm imp}(\mathbf{r})$ is the disorder potential, α is the SO coupling, $\vec{\sigma}$ is the vector of Pauli matrices, $\Psi(\mathbf{r})$ and $\Psi^\dagger(\mathbf{r})$ are spinor fields which respectively create and destroy electrons at position $\mathbf{r}$ and $\hat{a} = \vec{a}/|\vec{a}|$. Here we limit ourselves to the simplest case of Gaussian random disorder with "white noise" correlations, namely we set $\langle V_{\rm imp}(\mathbf{r})V_{\rm imp}(\mathbf{r}')\rangle_{\rm imp} = n_i v_{\rm imp}^2\delta(\mathbf{r}-\mathbf{r}')$ where $v_{\rm imp}$ and n_i denote respectively the scattering strength and the impurity density. In the absence of impurities, H gives an electronic spectrum, depicted in Fig.1, consisting of two bands with dispersion $E_p^s - E_0 = (p + sp_0)^2/(2m) - E_0$, where $p_0 = m\alpha$, $E_0 = m\alpha^2/2$ and $s = \pm 1$ denotes the eigenvalue of the helicity operator, S, defined as usual as $S = \hat{z}\cdot(\hat{p}\times\vec{\sigma})$. In the following we measure the Fermi energy, E_F, from the lower band edge, so that $E_F = E_0$ corresponds to the "Dirac point", $p = 0$, and the HD and DSO regimes are realised respectively for $E_F > E_0$ and $E_F < E_0$.

As already noted in [40], the onset of the DSO regime leads to a rather sharp change in density of states (DOS) at the Fermi level. Indeed, while for $E_F > E_0$ the DOS is constant, $N(E_F) = N_0 = m/(\pi\hbar^2)$, for $E_F < E_0$ it displays a van Hove singularity, $N(E_F) = N_0\sqrt{E_0/E_F}$ leading to a modification of the dependence of the density

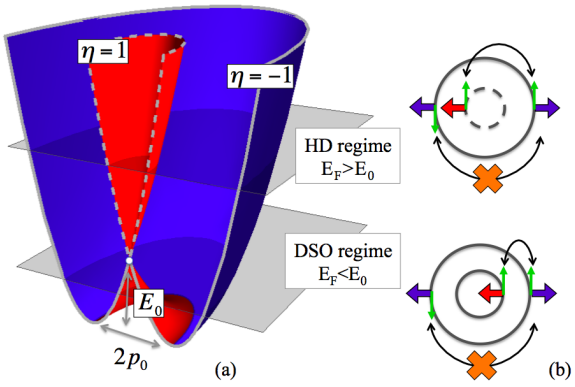

Figure 1: (Color online) (a): dispersion of the Rashba model. The solid/dashed contours and the red/blue colours denote respectively s and η. (b): Examples of allowed and forbidden back-scattering processes. Thick (red and blue) and thin green arrows denote the quasi-particle velocity $\vec{v}_{\mathbf{p}s}$ and the spin $\langle\vec{\sigma}\rangle_{\mathbf{p}s}$ of each state, respectively.

on the Fermi energy [40]:

$$n \simeq \begin{cases} N_0(E_F + E_0) & E_F > E_0 \\ 2N_0\sqrt{E_F E_0} & E_F < E_0. \end{cases} \tag{4}$$

In the presence of static diluted disorder, the singular behavior of the DOS reflects directly on the quasiparticles lifetime that, using Fermi golden rule (see *e.g.* Ref.[4]), can be cast as $\tau(E_p^s) = \mathcal{V}\,[\sum_{\mathbf{p}'s'} Q^{\mathbf{p}s}_{\mathbf{p}'s'}]^{-1}$, where $\mathcal{V}$ is the 2D volume of the sample and

$$Q^{\mathbf{p}s}_{\mathbf{p}'s'} = \pi n_i v_{imp}^2 (1 + ss'\hat{p}\cdot\hat{p}')\delta(E_p^s - E_{p'}^{s'}), \tag{5}$$

is the scattering kernel. Using Eqs. (4-5) one can easily show that the quasi-particle scattering time scales linearly with the density in the DSO regime, *i.e.*

$$\tau = \tau(E_F) = \begin{cases} \tau_0 & E_F > E_0 \\ \tau_0\sqrt{E_F/E_0} = \tau_0(n/n_0) & E_F < E_0, \end{cases} \tag{6}$$

where $\tau_0 = \hbar^2/(m n_i v_{imp}^2)$ denotes the quasi-particle scattering time in the absence of SO.

To explain the behavior of the conductivity across the different regimes, we start by recalling the definition of the velocity operator in the helicity basis,

$$[\vec{v}]_{ss'} = \vec{v}_{\mathbf{p}s}\delta_{ss'} - i\alpha s(1-\delta_{ss'})\hat{t}_p, \tag{7}$$

where $\vec{v}_{\mathbf{p}s} = \nabla_{\mathbf{p}} E_p^s = \hat{p}(p/m + s\alpha)$ denotes the quasi-particle velocity and $\hat{t}_p$ is defined as $\hat{t}_p = \{p_y/p, -p_x/p\}$. An important thing to underline here, general for any chiral system, is that in the presence of SO coupling also the velocity acquires a spin structure, which has a deep impact on the transport properties. As we discuss in more details below, to a first approximation the conductivity can be described within a standard semiclassical Boltzmann approach that only keeps the quasiparticle current, arising from the diagonal components of the velocity operator (7). In the relaxation time approximation at $T = 0$, σ_{dc} can be then estimated as

$$\sigma_{dc} \simeq \sigma_{dc}^{\mathrm{B}} = \frac{e^2}{2\mathcal{V}} \sum\nolimits_{\mathbf{p}s} \delta(E_F - E_p^s)|\vec{v}_{\mathbf{p}s}|^2 \tau_{ps}^{\mathrm{tr}} \tag{8}$$

where the transport scattering times τ_{ps}^{tr} satisfy the following equations [43]

$$\frac{\tau_{ps}^{\mathrm{tr}}}{\tau(E_p^s)} = 1 + \frac{1}{\mathcal{V}} \sum_{\mathbf{p}'s'} Q^{\mathbf{p}'s'}_{\mathbf{p}s} \frac{\vec{v}_{\mathbf{p}'s'}\cdot\vec{v}_{\mathbf{p}s}}{|\vec{v}_{\mathbf{p}s}|^2} \tau_{p's'}^{\mathrm{tr}}. \tag{9}$$

Using explicitly the definition of $Q^{\mathbf{p}'s'}_{\mathbf{p}s}$ (5), we introduce the transport helicity index $\eta = s(\hat{v}_{\mathbf{p}s}\cdot\hat{p}) \equiv \hat{z}\cdot(\vec{v}_{\mathbf{p}s} \times \langle\vec{\sigma}\rangle_{\mathbf{p}s}) = \pm 1$, that accounts for the reciprocal orientation of spin and velocity, and we recast Eq.(9) as follows:

$$\frac{\tau_\eta^{\mathrm{tr}}}{\tau} = 1 + \frac{n_i v_{\mathrm{imp}}^2}{4 v_F \hbar^2} \sum_{\eta'} \eta\eta' p_{\eta'} \tau_{\eta'}^{\mathrm{tr}}, \tag{10}$$

where $v_F = \sqrt{2mE_F}$ and $p_\eta = |mv_F - \eta\, p_0|$ are the Fermi momenta on the inner and outer Fermi surfaces. The above equation suggests that the index η can be used to efficiently classify the states at the Fermi level across the different regimes. In particular, as illustrated in Fig.1a, where the value of η is indicated by the red/blue colors of the surface, at $E_F > E_0$ η simply coincides with s, on the contrary, at $E_F < E_0$ η allows to distinguish between the two Fermi circles that have the same value of s but antiparallel quasi-particle velocities. Using this classification σ_{dc}^{B} can be cast as

$$\sigma_{dc}^{\mathrm{B}} = \frac{e^2 v_F}{4\pi} \sum\nolimits_\eta \tau_\eta^{\mathrm{tr}} p_\eta = \sum\nolimits_\eta \sigma_\eta, \tag{11}$$

where the transport scattering times τ_η^{tr} are given by the solution of Eqs. (10)

$$\tau_\eta^{\mathrm{tr}} = \tau\, p_\eta/\bar{p}_F, \tag{12}$$

with $\bar{p}_F = 1/2\sum_\eta p_\eta$, *i.e.* $\bar{p}_F = mv_F$ for $E_F > E_0$ and $\bar{p}_F = p_0$ for $E_F < E_0$. As one can easily check, Eqs.(11) and (12) yield Drude result (1) at $E_F > E_0$, and Eq.(2) in the DSO regime.

The physical relevance of η, as compared to the standard helicity, s, is evident in Fig.1b, where we show that spin conservation forbids back-scattering between states having the same value of η. What is more important, in the DSO regime the only allowed back-scattering processes reverse the sign of the quasi-particle velocity without changing the direction of momentum. These effects determine the density dependence of the scattering times (a) and of the conductivities (b) of the the majority ($\eta = -1$) and minority ($\eta = +1$) carriers shown in Fig.2. As one can see in Fig.2b, transport is in general

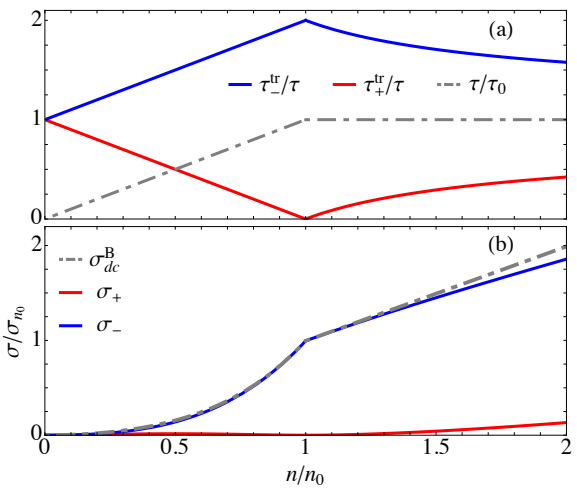

Figure 2: (Color online) (a) Density dependence of the ratio $\tau_\mp/\tau$ for the majority ($\tau_-^{\rm tr}$, solid blue line) and minority ($\tau_+^{\rm tr}$, solid red line) carriers, and of the ratio τ/τ_0 (dashed line). (b) Density dependence of Boltzmann dc conductivity σ_{dc}^B, and contribution $\sigma_\mp$ of the two types of carriers, in units of $\sigma_{n_0} = n_0 e^2 \tau_0/m$.

dominated by the majority carriers that, due to the suppression of backscattering have also the larger transport scattering time, $\tau_-^{\rm tr} > \tau > \tau_+^{\rm tr}$. Let us focus on the transport properties of majority and minority carriers across the different regimes. In the HD regime τ is a constant and $\tau_-^{\rm tr}/\tau$ increases as the density decreases due to the shrinking of the inner Fermi circle. At $n = n_0$, where only states with $\eta = -1$ are present, back-scattering is completely suppressed and one recovers $\tau_-^{\rm tr} = 2\tau$, like e.g. in graphene [42]. However, differently from graphene, as long as $n > n_0$ a compensation between SO effects on the velocity and on the transport scattering times of the two types of carriers restores the usual Drude conductivity, even for n very close to n_0. This result is non trivial: indeed, setting naively $\tau_\eta^{\rm tr} = \tau$ in Eq.(8), would lead to [43] $\sigma \simeq (n - n_0/2)\tau_0/m$ *i.e.* $\sigma < \sigma_{\rm Drude}$ even at $n > n_0$ [44]. On the other hand, as the system enters the DSO regime τ starts to decrease linearly as predicted by Eq. (6) and backscattering processes for the majority carriers are progressively restored. Both these effects quench $\tau_-^{\rm tr}$ as $n < n_0$, see Fig. 2a, leading to an overall sublinear behavior of the conductivity, see Fig. 2b.

A deeper insight on dc transport comes from the generalisation of Boltzmann approach to fully include quantum effects. To this end, we use Kubo linear response theory [1]. We start by noticing that, within the self-consistent Born approximation (SCBA), the retarded Green's function is diagonal in the helicity basis and it is given by the following matrix [1, 48],

$$\left[G^R(\mathbf{p},\omega)\right]_{ss'} = g_s^R(p,\omega)\delta_{ss'}, \tag{13}$$

where $g_s(p,\omega) = \left[\omega - E_p^s + E_F - \Sigma^R(\omega)\right]^{-1}$ denotes the Green function of electrons with helicity s. The self-energy $\Sigma^R(\omega) = n_i v_{\rm imp}^2/(2\mathcal{V})\sum_{\mathbf{p},s} g_s^R(p,\omega)$ is spin and momentum independent [1]. At zero frequency its imaginary part defines the elastic scattering rate of quasi-particles, $\Gamma = -{\rm Im}[\Sigma^R(0)] = n_i v_{\rm imp}^2\pi/(2\mathcal{V})\sum_{\mathbf{p},s}\mathcal{A}_s(p)$, where $\mathcal{A}_s(p) = -(1/\pi){\rm Im}g_s^R(p,\omega=0)$ is the spectral function of each helicity band. In Fig.3a we plot the numerical self-consistent Γ as a function of the ratio n/n_0 for different values of the SO coupling and we compare it with Boltzmann result $\Gamma_B = 1/(2\tau)$. As expected Boltzmann result is accurate for large n/n_0, where $\Gamma \ll E_F$ holds and one can approximate the spectral function as $\mathcal{A}_s(p) \simeq \delta(E_p^s - E_F)$, and its accuracy increases with increasing E_0/Γ_0. On the contrary, as E_F approaches the band edge, the DOS singularity is smeared by disorder and finite-band effects cut-off the divergence of Boltzmann result $\Gamma_B = \Gamma_0\sqrt{E_0/E_F}$ following from (6). In the extreme diluted limit, (shaded region in Fig.3a) Γ as given by the SCBA vanishes and the diffusive approximation breaks down [43].

Within linear response theory the conductivity is given by Kubo formula and, at $T = 0$, it is related to the on-shell current-current response function as follows [1]

$$\sigma_{dc} = \frac{\hbar}{2\pi}\left(P_{xx}^{AR} - {\rm Re}[P_{xx}^{RR}]\right), \tag{14}$$

where P_{xx}^{LM} is given by

$$P_{xx}^{LM} = \frac{1}{\mathcal{V}}\sum\nolimits_{\mathbf{p}} {\rm Tr}\left[j_x(\mathbf{p})G^L(\mathbf{p},0)J_x^{LM}(\mathbf{p})G^M(\mathbf{p},0)\right], \tag{15}$$

and the superscripts $L, M = A, R$ indicate advanced/retarded quantities. In the above equation $j_x(\mathbf{p})$ and $J_x^{LM}(\mathbf{p})$ denote the bare and dressed currents and they are in general represented by 2×2 matrices in the helicity space. In particular, $j_x(\mathbf{p}) = e{\rm v}_x$ is proportional to the bare velocity (7), while J_x has to be determined self-consistently [43] and it can be written as

$$\left[\vec{J}^{LM}(\mathbf{p})\right]_{ss'} = e\left[\vec{V}_{\mathbf{p}s}^{LM}\delta_{ss'} - i\tilde{\alpha}^{LM}s(1-\delta_{ss'})\hat{t}_p\right], \tag{16}$$

where $\vec{V}_{\mathbf{p}s}^{LM} = \mathbf{p}/m + s\tilde{\alpha}^{LM}\hat{p}$ denotes the dressed quasi-particle velocity. By comparing Eqs. (7) and (16) one sees that, as usual [1] in Kubo formalism the effects of scattering by impurities are encoded, *via* the vertex function $\tilde{\alpha}^{LM}$, in the renormalization of the velocity. As we show below, under appropriate conditions, these effects are equivalently accounted for in Boltzmann language by the transport scattering times.

The anomalous velocity $\tilde{\alpha}^{LM}$ also plays an important role in the spin-Hall effect [46]. In this context it was shown that, although $\tilde{\alpha}^{RA} = 0$ in the HD regime [36, 47, 49] and $\tilde{\alpha}^{RA} \neq 0$ in the DSO regime [48], in both regimes the spin-Hall conductivity vanishes. This result follows straightforwardly from the vanishing of $\tilde{\alpha}^{RA}$ in the HD

regime while it can be proven by an explicit calculation in the DSO regime [48].

Using Eqs.(7) and (16), the current response function (15) can be cast as the sum of inter- and intra-band terms: $P^{LM}_{xx} = P^{LM}_{\rm intra} + P^{LM}_{\rm inter}$, where

$$P^{LM}_{\rm intra} = \frac{e^2}{2\mathcal{V}} \sum\nolimits_{\mathbf{ps}} \vec{v}_{\mathbf{ps}} \cdot \vec{\mathrm{V}}^{LM}_{\mathbf{ps}} g^L_s(p,0) g^M_s(p,0) \quad (17)$$

$$P^{LM}_{\rm inter} = \frac{e^2}{2\mathcal{V}} \alpha\, \tilde{\alpha}^{LM} \sum\nolimits_{\mathbf{p}\, s\neq s'} g^L_s(p,0) g^M_{s'}(p,0). \quad (18)$$

From a numerical self-consistent solution of the self-energy and vertex equations, we calculate the fully quantum dc conductivity Eq.(26). The results are shown in Fig. 3(b), where we plot the conductivity as a function of the electronic density and of the SO coupling. Here we also plot Boltzmnann conductivity (blue lines) for two values of E_0, showing that Kubo results follow quite closely Boltzmann prediction.

The equivalence between the two approaches can be proven in the the limit of vanishingly small broadening of the spectral functions, $\Gamma \ll E_F$, where we can discard[1] the RR term in Eq. (26). Indeed by neglecting also the inter-band contribution to P^{RA}, relevant only at $n \simeq n_0$ where the spectral functions of the two chiral bands overlap, we can recast the conductivity as

$$\sigma_{dc} \simeq \frac{e^2}{4\mathcal{V}\Gamma} \sum\nolimits_{\mathbf{ps}} \vec{v}_{\mathbf{ps}} \cdot \vec{V}^{RA}_{\mathbf{ps}} \delta(E_F - E^s_p), \quad (19)$$

that, by direct comparison with (8), yields $\sigma_{dc} \simeq \sigma^B_{dc}$ provided that $\vec{V}^{RA}_{\mathbf{ps}} \simeq \tau^{tr}_{\mathbf{ps}} \vec{v}_{\mathbf{ps}}/\tau$. In the limit $\Gamma \ll E_F$ this relation is a straightforward consequence of the vanishing of $\tilde{\alpha}^{RA}$ for $E_F > E_0$ and it can be easily proved for $E_F < E_0$ using $\tilde{\alpha}^{RA} \simeq \alpha(1 - E_F/E_0)$ [43]. This shows in particular that on the Fermi circles $V_{\mathbf{ps}}/v_F = \tau^{\rm tr}_\eta/\tau$.

The deviations between Boltzmann and Kubo results are better seen in Fig. 3c, where we compare the corresponding mobilities, respectively defined as $\mu_B = \sigma^{\rm B}_{dc}/(en)$ and $\mu_t = \sigma_{dc}/(en)$, and they can be ultimately ascribed to two factors. First, finite-band effects, that are mostly relevant for $n \lesssim 0.3 n_0$ and are responsible for the deviations of Γ from Γ_B, shown in Fig. 3a, and for the relevance of RR terms [43] that in turn imply that for small densities μ_t tends to saturate, in contrast to μ_B. Second, inter-band terms that are mostly relevant at $n \simeq n_0$ and give a smoothening of dependence of μ_t on n. This effect could be also captured by replacing the semiclassical Boltzmann equation with a fully quantum kinetic equation that includes also the off-diagonal components of the velocity operator (7) and of the non-equilibrium density-matrix in the helicity space. This allows one to account, in the presence of external fields, for the coherent superpositions of states with different helicities, as explained *e.g.* in Refs. [9, 10, 33, 50].

In conclusion, we have shown that in Rashba 2DEGs SO coupling entails an unconventional dc conductivity,

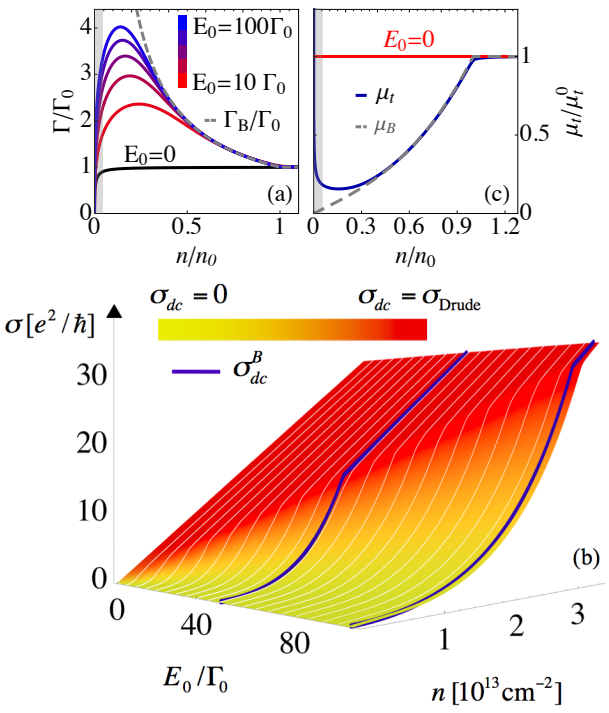

Figure 3: (Color online) (a): Scattering rate in units of Γ_0 as a function of n/n_0 for different E_0. The dashed line shows $\Gamma_{\rm B} = 1/2\tau$ (Eq. (6)). (b)Numerical dc conductivity (Eq. (26)) as a function of E_0/Γ_0 and n for $\Gamma_0 = 0.5$meV and $m = 0.7 m_e$ (as appropriate e.g. for $LaAlO_3/SrTiO_3$ interfaces [24]). The blue lines show Boltzmann conductivity for $E_0 = 50$ and $100\,\Gamma_0$ (c) Mobility μ_t (solid line) normalized to $\mu^0_t = e/(2\hbar\Gamma_0 m)$, compared with Boltzmann's $\mu_{\rm B}$ (dashed line). Shaded areas in (a) and (c) denote the low-density regions beyond the diffusive approximation.

strongly dependent on the density and on the SO-coupling strength. The experimental verification of our results requires the condition for diffusive transport ($E_F \gg \Gamma$) to be fulfilled in the DSO regime ($E_0 > E_F$): this ultimately implies $E_0 > E_F \gg \Gamma$. The conductivity anomalies in the DSO regime can then be accessible experimentally in relatively clean ($\Gamma_0 \sim 1$ meV) samples of the strong-Rashba materials mentioned in the Introduction (see Refs.[3–32]), where $E_0 \approx 10 - 140$ meV and $m \approx 0.2 - 0.7 m_e$, corresponding to electron densities $n_0 \approx 0.6 - 8 \times 10^{13}$ cm^{-2} [53]. Finally, we also remark that the large value of E_0 in these systems guarantees that our zero-temperature results will provide a good description for real materials up to temperature scales $k_B T \sim E_0$. In addition, the occurrence of the DSO anomalies at relatively large densities $n \simeq n_0$ justifies also neglecting of electron-electron interactions, even though a full understanding of the conductivity anomalies in the diluted regime where interactions become relevant is certainly an interesting topic for

future investigation. *Acknowledgements* We gratefully acknowledge fruitful discussions with S. Caprara, C. Castellani, M. Grilli and R. Raimondi. We acknowledge financial support by Italian MIUR under projects FIRB-HybridNanoDev-RBFR1236VV, PRIN-RIDEIRON-2012X3YFZ2, Premiali-2012 AB-NANOTECH, by the European project FP7-PEOPLE-2013-CIG "LSIE_2D".

[1] D. D. Awschalom and M. J. Flatté, Nature Physics **3**, 153 - 159 (2007).
[2] A. Manchon, H. C. Koo, J. Nitta, S. M. Frolov and R. A. Duine Nature Materials **14**, 871 (2015).
[3] C. R. Ast, J. Henk, A. Ernst, L. Moreschini, M. C. Falub, D. Pacile', P. Bruno, K. Kern, and M. Grioni, Phys. Rev. Lett. **98**, 186807 (2007).
[4] C. R. Ast, D. Pacilé, L. Moreschini, M. C. Falub, M. Papagno, K. Kern, M. Grioni, J. Henk, A. Ernst, S. Ostanin, and P. Bruno, Phys. Rev. B **77**, 081407 (2008).
[5] I. Gierz, T. Suzuki, E. Frantzeskakis, S. Pons, S. Ostanin, A. Ernst, J. Henk, M. Grioni, K. Kern, and C. R. Ast, Phys. Rev. Lett. **103**, 046803 (2009).
[6] H. Mirhosseini, A. Ernst, S. Ostanin, and J. Henk, J. Phys.: Condens. Matter **22**, 385501 (2010).
[7] K. Yaji, Y. Ohtsubo, S. Hatta, H. Okuyama, K. Miyamoto, T. Okuda, A. Kimura, H. Namatame, M. Taniguchi, and T. Aruga, Nature Comm. **1**, 17 (2010).
[8] D. V. Gruznev, L. V. Bondarenko, A. V. Matetskiy, A. A. Yakovlev, A. Y. Tupchaya, S. V. Eremeev, E. V. Chulkov, J.-P. Chou, C.-M. Wei, M.-Y. Lai, Y.-L. Wang, A. V. Zotov, and A. A. Saranin, Sci. Rep. **4**, 4742 (2014).
[9] J. C. Rojas Sánchez, L. Vila, G. Desfonds, S. Gambarelli, J. P. Attané, J. M. De Teresa, C. Magén and A. Fert, Nat. Comm. **4** 2944 (2013).
[10] S. V. Eremeev, I. A. Nechaev, Y. M. Koroteev, P. M. Echenique, and E. V. Chulkov, Phys. Rev. Lett. **108**, 246802 (2012).
[11] M. Bahramy, B.-J. Yang, R. Arita, and N. Nagaosa, Nature Comm. **3**, 679 (2012).
[12] M. Sakano, M. Bahramy, A. Katayama, T. Shimojima, H. Murakawa, Y. Kaneko, W. Malaeb, S. Shin, K. Ono, H. Kumigashira, R. Arita, N. Nagaosa, H. Y. Hwang, Y. Tokura, and K. Ishizaka, Phys. Rev. Lett. **110**, 107204 (2013).
[13] X. Xi, C. Ma, Z. Liu, Z. Chen, W. Ku, H. Berger, C. Martin, D. B. Tanner, and G. L. Carr, Phys. Rev. Lett. **111**, 155701 (2013).
[14] Y. L. Chen, M. Kanou, Z. K. Liu, H. J. Zhang, J. A. Sobota, D. Leuenberger, S. K. Mo, B. Zhou, S-L. Yang, P. S. Kirchmann, D. H. Lu, R. G. Moore, Z. Hussain, Z. X. Shen, X. L. Qi and T. Sasagawa, Nature Physics **9**, 704 (2013).
[15] L. Ye, J. G. Checkelsky, F. Kagawa, Y. Tokura, Phys. Rev. B **91** 201104 (2015).
[16] Fei-Xiang Xiang, Xiao-Lin Wang, Menno Veldhorst, Shi-Xue Dou, and Michael S. Fuhrer, Phys. Rev. B **92**, 035123 (2015).
[17] Y. Gui, C. Becker, N. Dai, J. Liu, Z. Qiu, E. Novik, M. Schaefer, X. Shu, J. Chu, H. Buhmann, and et al., Phys. Rev. B **70**, 115328 (2004).
[18] A. Ohtomo and H. Y. Hwang, Nature **427**, 423 (2004).
[19] N. Reyren, S. Thiel, A. D. Caviglia, L. F. Kourkoutis, G. Hammerl, C. Richter, C. W. Schneider, T. Kopp, A.-S. Ruetschi, D. Jaccard, and et al., Science **317**, 1196 (2007).
[20] A. D. Caviglia, S. Gariglio, N. Reyren, D. Jaccard, T. Schneider, M. Gabay, S. Thiel, G. Hammerl, J. Mannhart, and J.-M. Triscone, Nature **456**, 624 (2008).
[21] C. Bell, S. Harashima, Y. Kozuka, M. Kim, B. G. Kim, Y. Hikita, and H. Y. Hwang, Phys. Rev. Lett. **103**, 226802 (2009).
[22] A. D. Caviglia, M. Gabay, S. Gariglio, N. Reyren, C. Cancellieri, and J.-M. Triscone, Phys. Rev. Lett. **104**, 126803 (2010).
[23] M. Ben Shalom, M. Sachs, D. Rakhmilevitch, A. Palevski, and Y. Dagan, Phys. Rev. Lett. **104**, 126802 (2010).
[24] J. Biscaras, N. Bergeal, S. Hurand, C. Grossetete, A. Rastogi, R. C. Budhani, D. LeBoeuf, C. Proust, and J. Lesueur, Phys. Rev. Lett. **108**, 247004 (2012).
[25] S. Seri, M. Schultz, and L. Klein, Phys. Rev. B **86**, 085118 (2012).
[26] A. Joshua, J. Ruhman, S. Pecker, E. Altman, and S. Ilani, Proc. Nat. Acad. Sci. **110**, 9633 (2013).
[27] S. Hurand, A. Jouan, C. Feuillet-Palma, G. Singh, J. Biscaras, E. Lesne, N. Reyren, A. Barthlmy, M. Bibes, J. E. Villegas, C. Ulysse, X. Lafosse, M. Pannetier-Lecoeur, S. Caprara, M. Grilli, J. Lesueur and N. Bergeal, Sci. Rep. **5** 12751 (2015).
[28] Q. Liu, Y. Guo, and A. J. Freeman, Nano Lett. **13**, 5264 (2013).
[29] J. Biscaras, S. Hurand, C. Feuillet-Palma, A. Rastogi, R. C. Budhani, N. Reyren, E. Lesne, J. Lesueur, and N. Bergeal, Sci. Rep. **4**, 6788 (2014).
[30] Z. Zhong, L. Si, Q. Zhang, W.-G. Yin, S. Yunoki, and K. Held, Adv. Mater. Interfaces **2**, 201400445 (2015).
[31] Z. Zhong, A. Tóth, and K. Held Phys. Rev. B **87** 161102 (2013).
[32] A. Joshua, S. Pecker, J. Ruhman, E. Altman, and S. Ilani Nature Comm. **3**, 1129 (2012).
[33] A. V. Khaetskii, Phys. Rev. Lett. **96**, 056602 (2006).
[34] R. Raimondi, M. Leadbeater, P. Schwab, E. Caroti, and C. Castellani, Phys. Rev. B **64**, 235110 (2001).
[35] P. Schwab and R. Raimondi, Eur. Phys. J. B **25**, 483 (2002).
[36] R. Raimondi and P.Schwab, Phys. Rev. B **71**, 033311 (2005).
[37] Amit Agarwal, Stefano Chesi, T. Jungwirth, Jairo Sinova, G. Vignale, and Marco Polini Phys. Rev. B 83, 115135 (2011).
[38] D. Bercioux and P. Lucignano, Report on Progress in Physics 78, 106001 (2015).
[39] E. I. Rashba and Y. A Bychkov, JETP Letters **39**, 66 (1984).
[40] E. Cappelluti, C. Grimaldi, and F. Marsiglio, Phys. Rev. Lett. **98**, 167002 (2007).
[41] J. M. Ziman, *Principles of the Theory of Solids* (Cambridge University Press, Cambridge, United Kingdom, 1972).
[42] See e.g. A. H. Castro Neto, F. Guinea, N. M. R. Peres, K. S. Novoselov, A. K. Geim, Rev. Mod. Phys. **81**, 109 (2009) and references therein.
[43] See Supplementary Material which includes Refs.[2, 3, 7] for more details.

[44] Zhou Li, F. Marsiglio and J. P. Carbotte, Sc. Rep. **3**, 1 (2013).
[45] G. D. Mahan, *Many-Particle Physics* (Springer, Berlin-Heidelberg, 2000).
[46] Dyakonov, M., and V. I. Perel, ZhETF Pis. Red. **13**, 657 (1971).
[47] R. Raimondi, P. Schwab, C. Gorini, and G. Vignale, Annalen der Physik **524**, 153 (2011).
[48] C. Grimaldi, E. Cappelluti, and F. Marsiglio, Phys. Rev. B **73**, 081303 (2006).
[49] G. Vignale, J. Supercond. Nov. Magn. **23**, 3 (2010).
[50] M. I. D'yakonov and A. V. Khaetskii, Zh. Eksp. Teor. Fiz. **86**, 1843 (1984)
[51] A. V. Shytov, E. G. Mishchenko, H.-A. Engel, and B. I. Halperin Phys. Rev. B **73**, 075316 (2006).
[52] R. Raimondi, C. Gorini P.Schwab M. Dzierzawa, Phys. Rev B **74**, 035340 (2006).
[53] A concrete example is given in Fig. 3 where we chose parameter values [27] appropriate for LAO/STO interfaces. An even more favorable situation is found on the surface of BiTeI where $E_0 \approx 0.1$ eV [12], and the electron mass $m \sim 0.2\, m_e$[13], leading to $n_0 = 1.9 \times 10^{13}\mathrm{cm}^{-2}$. Similarly, in surface alloys, (see *e.g.* Ref. [5]), E_0 and m are approximately 140 meV and $0.7m_e$ predicting a DSO regime for $n \leq n_0 \sim 8 \times 10^{13}\mathrm{cm}^{-2}$. We remark that both in surface alloys [4] and in bulk BiTeI [16] the regime $E_F \lesssim E_0$ has been already demonstrated to be accessible experimentally.
[54] H. Bruus and C. Flenshberg, *Many-Body Quantum Theory in Condensed Matter Physics* (Oxford University Press, New York, 2004).
[55] A. Knigavko and J. P. Carbotte Phys. Rev. B 72, 035125 (2005).
[56] N. A. Sinitsyn, A. H. MacDonald, T. Jungwirth, V. K. Dugaev, and Jairo Sinova, Phys. Rev. B 75, 045315 (2007)

Supplemental Material to "Unconventional dc Transport in Rashba Electron Gases"

HELICITY EIGENSTATES BASIS

To fix the notation, let us start by giving some details on the helicity eigenstates basis. The helicity operator is defined as $S = [\hat{p} \times \vec{\sigma}]_z$ and its eigenstates, $|\mathbf{k}s\rangle$, with $s = \pm 1$, satisfy the relation $S|\mathbf{k}\pm\rangle = \pm|\mathbf{k}\pm\rangle$. A simple calculation shows in particular that $|\mathbf{k}\pm\rangle$ can be expressed in terms of the standard spin eigenstates, $|\mathbf{k}\uparrow\rangle$ and $|\mathbf{k}\downarrow\rangle$, as $|\mathbf{k}\pm\rangle = (\exp(-i\theta_{\mathbf{k}})|\mathbf{k}\uparrow\rangle \pm i|\mathbf{k}\downarrow\rangle)/\sqrt{2}$ with $\theta_{\mathbf{k}} = \arctan(k_y/k_x)$. Consequently, the matrix $U_{\mathbf{k}}$ which implements the rotation from the spin to the helicity eigenstates basis has the form

$$U_{\mathbf{k}} = \frac{1}{\sqrt{2}} \begin{pmatrix} e^{-i\theta_{\mathbf{k}}} & e^{-i\theta_{\mathbf{k}}} \\ i & -i \end{pmatrix}. \tag{20}$$

In the basis spanned by the states $|\mathbf{k}s\rangle$ the total Hamiltonian (Eq. (3) in main text) can be recast as follows:

$$H = \sum_{\mathbf{k}} c^{\dagger}_{\mathbf{k}} H_k \, c_{\mathbf{k}} + \sum_{\mathbf{q},\mathbf{k}} V_{\rm imp}(\mathbf{q}) c^{\dagger}_{\mathbf{k}+\mathbf{q}} U^{\dagger}_{\mathbf{k}+\mathbf{q}} U_{\mathbf{k}} c_{\mathbf{k}} \tag{21}$$

where $c_{\mathbf{k}} = (c_{\mathbf{k}+}, c_{\mathbf{k}-})$ and $c^{\dagger}_{\mathbf{k}} = (c^{\dagger}_{\mathbf{k}+}, c^{\dagger}_{\mathbf{k}-})$ are spinor creation and annihilation operators, H_k is the Hamiltonian of the clean Rashba model, *i.e.* $H_k = \mathrm{diag}(E^+_k - E_0, E^-_k - E_0)$ with $E^{\pm}_k = (k \pm p_0)^2/(2m)$, $p_0 = m\alpha$ and $V_{\rm imp}(\mathbf{q})$ denotes the Fourier transform of the impurity potential, $V_{\rm imp}(\mathbf{q}) = 1/\mathcal{V} \sum_j e^{i\mathbf{q}\cdot\mathbf{R}_j} v_{\rm imp}$. Differently from the main text, in this Supplementary Material where not differently specified we use units $\hbar = e = 1$.

GREEN'S FUNCTION

The Green's function obeys the standard Dyson equation: $G^{-1} = \left(G^0\right)^{-1} - \Sigma$, where G^0 is the Green's function of the Rashba model in the absence of disorder and Σ is the self-energy. Specifically, in the helicity eigenstates basis, G^0 has the form

$$[G^0]_{\alpha\beta} = (i\varepsilon_l - E^{\alpha}_p + E_F)^{-1}\delta_{\alpha\beta}$$

where ε_l is a fermionic Matsubara frequency, and from now on we set the zero of the energy to $-E_0$. Thus, as in the main text, the dominant spin-orbit (DSO) regime is identified by $E_F < E_0$. Within the self-consistent Born approximation (SCBA), $\Sigma = \Sigma(\mathbf{p}, i\varepsilon_n)$ is determined by solving the following equation

$$\Sigma(\mathbf{k}, i\epsilon_n) = \frac{n_i v^2_{\rm imp}}{\mathcal{V}} \sum\nolimits_{\mathbf{p}} U^{\dagger}_{\mathbf{p}} U_{\mathbf{k}} G(\mathbf{p}, i\epsilon_n) U^{\dagger}_{\mathbf{k}} U_{\mathbf{p}} \tag{22}$$

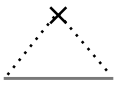

Figure 4: Wigwam diagrams which describe the self-energy within Born approximation. The solid line correspond to the dressed Green function, G, while the crosses indicate averaging over disorder [1, 2].

which corresponds the "wigwam diagram" depicted in Fig. 4 as described *e.g.* in Refs [1, 2]. Note that in the helicity basis to each impurity-scattering vertex, changing the electron momentum from $\mathbf{k}$ to $\mathbf{p}$, one has to associate the spin rotation $U^{\dagger}_{\mathbf{p}} U_{\mathbf{k}}$. Equation (22) admits a momentum- and spin- independent solution. Indeed, assuming $[\Sigma(\mathbf{p}, i\epsilon_n)]_{\alpha\beta} = \Sigma(i\epsilon_n)$, the momentum dependent part on the r.h.s. of this equation averages away. Within SCBA the Green's function $G(\mathbf{p}, i\epsilon_n)$ is thus represented by the following diagonal matrix in the helicity eigenstates basis:

$$[G(\mathbf{p}, i\varepsilon_l)]_{\alpha\beta} = (i\varepsilon_l - E^{\alpha}_p + E_F - \Sigma(i\epsilon_l))^{-1}\delta_{\alpha\beta}. \tag{23}$$

By analytical continuation to real frequencies of Eq. (22) (see *e.g.* [2]) we obtain the following self-consistent equations for the scattering rate Γ

$$\Gamma = -\mathrm{Im}[\Sigma^R(0)] = \frac{n_i v^2_{\rm imp} \Gamma}{2\mathcal{V}} \sum_{\mathbf{p}} \left[|g^R_+(p,0)|^2 + |g^R_-(p,0)|^2\right] \tag{24}$$

and the retarded self-energy $\Sigma^R(\omega)$

$$\Sigma^R(\omega) = \frac{n_i v^2_{\rm imp}}{2\mathcal{V}} \sum\nolimits_{\mathbf{p}s} g^R_s(p,\omega)\theta(p_c - p) \tag{25}$$

where $g^R_{\pm}(p,\omega) = \left[\omega - E^{\pm}_p + E_F - \Sigma^R(\omega)\right]^{-1}$ is the Green's function of each chiral eigenstate. To simulate a finite Brillouin zone, in Eq. (25) we introduced an upper momentum cut-off, p_c. The latter is needed, in particular, to regularize the real part of the self-energy, $\mathrm{Re}[\Sigma^R(\omega)]$, which would otherwise diverge logarithmically at the band edge, see *e.g.* Ref.[3]. In these regards, we notice that, contrarily to what happens in standard half-filled systems where $\mathrm{Re}[\Sigma^R(\omega)]$ is approximately ω-independent and it can be absorbed in a redefinition of the Fermi level, in the low-doping regime investigated here $\mathrm{Re}[\Sigma^R(\omega)]$ acquires a non-trivial frequency dependence. We thus need to calculate self-consistently both $\mathrm{Re}[\Sigma^R(\omega)]$ and $\mathrm{Im}[\Sigma^R(\omega)]$. Such self-consistent solution identifies the elastic scattering rate, $\Gamma = -\mathrm{Im}[\Sigma^R(0)]$ and the renormalized density of states

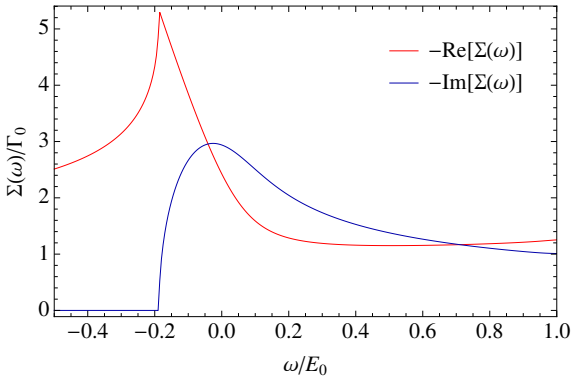

Figure 5: Structure of the real and imaginary part of the self-energy close to the lower band-edge for $E_0 = 40\Gamma_0$.

(DOS) $N(E) = -\frac{1}{\pi\mathcal{V}}\sum_{\mathbf{p}} \mathrm{Im}[G_R(\mathbf{p}, E)]$. The electronic density at $T = 0$ is given by $n = \int_{-\infty}^{E_F} N(E)dE$. At low doping the impurities lead to a smearing of the van-Hove singularity in the DOS, which reflects in the behavior of the scattering rate Γ, as described in the main text (Fig. 3a). In addition, the presence of impurities gives a shift, Δ_{edge}, of the lower band edge, so that the lower "effective" band edge where $n = 0$ is identified by $\tilde{E}_F = E_F + \Delta_{\mathrm{edge}} = 0$.In Fig.5, as an example we show the structure of the real and imaginary parts of the self-energy as functions of the frequency, for frequencies close to the lower band-edge, located at $E_F = -\Delta_{\mathrm{edge}}$. Notice that these two quantities are connected by Kramers-König relations.

DC CONDUCTIVITY FROM DIAGRAMMATIC PERTURBATION THEORY

Current response function

Within SCBA the static conductivity is given by Eq.(14) of the manuscript, that we report here for convenience

$$\sigma_{dc} = \frac{1}{2\pi}\left(P^{AR}_{xx} - \mathrm{Re}[P^{RR}_{xx}]\right). \tag{26}$$

The derivation of the above equation in the absence of spin-orbit coupling is standard textbooks material (see *e.g.* Refs. [1, 2]) and, since it does not change in the presence of spin-orbit coupling, we do not review it here.

By applying diagrammatic perturbation theory, one easily sees that the calculation of σ_{dc} implies the summation of all ladder diagrams shown in Fig. 6. This in turn corresponds to calculate the following current-

Figure 6: Ladder diagrams describing the conductivity within Born approximation. Solid lines and empty circles represent respectively $G(\mathbf{p}, i\varepsilon_l)$ and $j_x(\mathbf{p})$.

current response function in Matsubara frequencies:

$$P_{xx}(i\varepsilon_l, i\varepsilon_{l+n}) = \frac{1}{\mathcal{V}}\sum_{\mathbf{p}} \mathrm{Tr}\left\{G(\mathbf{p}, i\varepsilon_l) j_x(\mathbf{p}) G(\mathbf{p}, i\varepsilon_{l+n}) \cdot \right. \\ \left. \cdot \; J_x(\mathbf{p}, i\varepsilon_l, i\varepsilon_{l+n})\right\} \tag{27}$$

where j_x is the bare velocity operator introduced in the main text. We recall that in the helicity basis $j_x = e\mathrm{v}_x$ is represented by the following matrix:

$$\mathrm{v}_x = \frac{p_x}{m}\sigma_0 + \alpha\cos\theta_{\mathbf{p}}\sigma_z + \alpha\sin\theta_{\mathbf{p}}\sigma_y \tag{28}$$

where σ_0 is the 2×2 identity matrix and σ_i with $i = x, y, z$ are the Pauli matrices. The renormalized charge current $J_x(\mathbf{p}, i\varepsilon_l, i\varepsilon_m)$ satisfies the diagrammatic equation shown in Fig. 7 that in helicity space can be written as

$$J_x(\mathbf{k}, i\varepsilon_l, i\varepsilon_m) = j_x(\mathbf{k}) + \frac{n_i v_{\mathrm{imp}}^2}{\mathcal{V}}\sum_{\mathbf{p}} \Big[U^\dagger_{\mathbf{k}} U_{\mathbf{p}} G(\mathbf{p}, i\varepsilon_l)\cdot \\ J_x(\mathbf{p}, i\varepsilon_l, i\varepsilon_m) G(\mathbf{p}, i\varepsilon_m) U^\dagger_{\mathbf{p}} U_{\mathbf{k}}\Big] \tag{29}$$

Before coming to the solution of the above equation, we remark, that, as usual [2], the AR and RR response functions appearing in Eq.(26) correspond respectively to $P_{xx}(0 - i\delta, 0 + i\delta)$ and $P_{xx}(0 + i\delta, 0 + i\delta)$.

As it can be easily verified, by symmetry arguments one finds that J_x has the same matrix structure of the bare current (28), so that we can write:

$$J_x(\mathbf{k}, i\epsilon_l, i\epsilon_m) = \frac{p_x}{m}\sigma_0 + \tilde{\alpha}\cos\theta\sigma_z + \tilde{\alpha}\sin\theta\sigma_y \tag{30}$$

where $\tilde{\alpha}(i\varepsilon_l, i\varepsilon_m)$ satisfies the following self-consistent equation:

$$\tilde{\alpha} = \alpha + \frac{n_i v_{\mathrm{imp}}^2}{2}\sum_{\mathbf{p}} \mathrm{Tr}\big[U^\dagger_{\mathbf{p}}\sigma_y U_{\mathbf{p}} G(\mathbf{p}, i\varepsilon_l)\cdot \\ \cdot J_x(\mathbf{p}, i\varepsilon_l, i\varepsilon_m)\, G(\mathbf{p}, i\varepsilon_m)\big]. \tag{31}$$

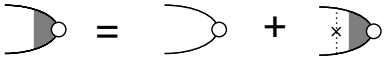

Figure 7: Diagrams describing renormalization of the charge current vertex.

Equation (31) can be solved explicitly to obtain to the following result for the renormalized anomalous vertex:

$$\tilde{\alpha}(i\varepsilon_l, i\varepsilon_m) = \frac{\alpha + \alpha_0(i\varepsilon_l, i\varepsilon_m)}{1 - A(i\varepsilon_l, i\varepsilon_m)} \tag{32}$$

where we introduced the quantities $A(i\varepsilon_l, i\varepsilon_m)$ and $\alpha_0(i\varepsilon_l, i\varepsilon_m)$ given by:

$$A(i\varepsilon_l, i\varepsilon_m) = \frac{n_i v_{\rm imp}^2}{4\mathcal{V}} \sum_{\mathbf{k}ss'} g_s(k, i\varepsilon_l) g_{s'}(k, i\varepsilon_m), \tag{33}$$

$$\alpha_0(i\varepsilon_l, i\varepsilon_m) = \frac{n_i v_{\rm imp}^2}{4\mathcal{V}} \sum_{\mathbf{k}s} \frac{k}{m} s\, g_s(k, i\varepsilon_l) g_s(k, i\varepsilon_m). \tag{34}$$

By replacing Eqs.(28) and (30) in Eq. (27), we arrive at the following expression for the correlation function $P_{xx}(i\varepsilon_l, i\varepsilon_m)$,

$$P_{xx}(i\varepsilon_l, i\varepsilon_m) = P_0(i\varepsilon_l, i\varepsilon_m) + \frac{m\left[(\alpha + \tilde{\alpha})\,\alpha_0 + \alpha\,\tilde{\alpha}\,A\right]}{\Gamma_0}. \tag{35}$$

On the r.h.s. of the above equation the frequency dependences of $\tilde{\alpha}$, α_0 and A, defined in Eqs.(31-34), is implied and we introduced the function $P_0(i\varepsilon_l, i\varepsilon_m)$,

$$P_0(i\varepsilon_l, i\varepsilon_m) = \frac{1}{2\mathcal{V}} \sum_{\mathbf{k}s} \frac{k^2}{m^2} g_s(k, i\varepsilon_l) g_s(k, i\varepsilon_m), \tag{36}$$

that in the absence of Rashba coupling yields the only non-vanishing contribution to the conductivity.

Once the analytical continuation is performed, Eq. (35) is equivalent to Eqs. (17-18) of the main text. This can be easily seen by inserting in Eq. (35) the explicit expression of A, α_0 and P_0, given above. One then finds that $P_{xx}^{LM}(0,0)$ can be recast as

$$P_{xx}^{LM} = \frac{1}{2\mathcal{V}} \sum_{\mathbf{p}} \Big\{ \left[\left(\frac{p^2}{m^2} + \alpha\tilde{\alpha}^{LM} \right) (g_+^L g_+^M + g_-^L g_-^M) \right] + \frac{p(\alpha + \tilde{\alpha})}{m} (g_+^L g_+^M - g_-^L g_-^M) + \alpha\tilde{\alpha}^{LM} (g_+^L g_-^M + g_-^L g_+^M) \Big\}.$$

From the above equation we see P_{xx} is the sum of an inter- and intra-band contribution, *i.e.*

$$P_{xx}^{LM} = \frac{1}{2\mathcal{V}} \sum_{\mathbf{p}} \Big\{ \sum_s \left[\Big(\frac{p}{m} + s\alpha \Big) \Big(\frac{p}{m} + s\tilde{\alpha}^{LM} \Big) g_s^L g_s^M \right] + + \alpha\tilde{\alpha}^{LM} \sum_{s \neq s'} g_s^L g_{s'}^M \Big\} \equiv P_{\rm intra}^{LM} + P_{\rm inter}^{LM}. \tag{37}$$

Eventually, since $(\frac{p}{m} + s\alpha)(\frac{p}{m} + s\tilde{\alpha}^{LM}) \equiv \vec{v}_{\mathbf{p}s} \cdot \vec{V}_{\mathbf{p}s}^{LM}$ we arrive at Eq. (18) of the main text.

Analytic approximations in the weak-disorder limit

Starting from the above results in this section we derive approximate analytical expressions for the renormalized vertex and the conductivity. We assume that we are in the weak-disorder limit (WDL), where we can (i) approximate the spectral functions with a delta, *i.e.* set $\mathcal{A}_\pm(p,0) = (\Gamma/\pi)|g_+^R(p,0)|^2 = \delta(E_{\mathbf{p}}^\pm - E_F)$; (ii) neglect the RR contributions.

The WDL approximation for $\tilde{\alpha}^{RA}$ can be derived starting from the analytic continuation of Eqs.(32-34). Performing the angular integral, A^{RA} and α_0^{RA} can be then cast as

$$\alpha_0^{RA}(0,0) = \frac{n_i v_{\rm imp}^2}{8m\pi} \int_0^\infty p^2 \left[|g_+^R(p,0)|^2 - |g_-^R(p,0)|^2 \right] dp, \tag{38}$$

$$A^{RA} = \frac{n_i v_{\rm imp}^2}{8\pi} \int_0^\infty p\, |g_+^R(p,0) + g_-^R(p,0)|^2 dp. \tag{39}$$

The latter equation can be simplified using the self-consistent self-energy equation to obtain:

$$A^{RA}(0,0) = 1/2 + \frac{n_i v_{\rm imp}^2}{4\pi} \int_0^\infty p\, {\rm Re}\big[g_+^R(p,0)\, g_-^R(p,0) \big]\, dp. \tag{40}$$

Approximating the spectral functions with a delta, as stated above, we immediately see that, except in a small density range around $E_F \simeq E_0$, we can neglect the second term and the r.h.s. of Eq.(40), since there is no overlap between the two-chiral bands and we obtain $A^{RA}(0,0) = 1/2$. In the same approximation, setting $\xi_p^\pm = E_p^\pm - E_F$, we can write $\alpha_0^{RA}(0,0)$ as follows

$$\alpha_0^{RA}(0,0) = \frac{n_i v_{\rm imp}^2}{8m\Gamma v_F} \int p^2 \left[\delta(\xi_p^+) - \delta(\xi_p^-) \right] dp\,, \tag{41}$$

which leads to

$$\alpha_0^{RA}(0,0) \simeq -\frac{\Gamma_0}{4m^2 v_F \Gamma} \cdot \begin{cases} (p_-^2 - p_+^2) & E_F > E_0 \\ (p_+^2 + p_-^2) & E_F < E_0 \end{cases} \tag{42}$$

with $\Gamma_0 = n_i v_{\rm imp}^2 m/2$. We recall that here, as in the main text, $p_\pm$ are the momenta on the inner and outer Fermi surface, so that their subscripts refer to the value of the transport helicity η, introduced in the main text in the context of Boltzmann transport. The sign change on the r.h.s. of Eq.(42) is thus due to the fact that for $E_F > E_0$ the two contributions come from the two chiral bands in Eq. (41), while for $E_F < E_0$ only the E_p^- band contributes, with a two-folded Fermi surface. Using the explicit expression $p_\pm$, *i.e.*

$$p_\pm^{E_F > E_0} = m v_F \mp p_0 \quad \text{and} \quad p_\pm^{E_F < E_0} = p_0 \mp m v_F. \tag{43}$$

with $v_F = \sqrt{2E_F/m}$, we eventually obtain:

$$\alpha_0^{RA}(0,0) \simeq \begin{cases} -\alpha & E_F > E_0 \\ -(E_0 + E_F)/p_0 & E_F < E_0 \end{cases} \tag{44}$$

Here we also used the WDL results for Γ, that can be derived from Eq. (24) in the WDL where $|g_\pm^R(p,0)|^2 =$

$(\pi/\Gamma)\delta(E^{\pm}_{\mathbf{p}s} - E_F)$ as

$$\Gamma^{WDL} = \begin{cases} \Gamma_0 & E_F > E_0 \\ \Gamma_0\sqrt{E_0/E_F} = \Gamma_0 p_0/(m v_F) & E_F < E_0 \end{cases} \tag{45}$$

that coincides with the Boltzmann result from Eq. (6) of the main text. By replacing the result (44) into Eq. (32), along with $A^{RA}(0,0) = 1/2$, we then obtain the estimate of $\tilde{\alpha}^{RA}$ quoted in the main text, i.e.

$$\alpha^{RA}(0,0) \simeq \begin{cases} 0 & E_F > E_0 \\ \alpha(1 - E_F/E_0) & E_F < E_0 \end{cases} \tag{46}$$

Let us now discuss the analytic approximation of the conductivity. As discussed in main text in the WDL we can put

$$\sigma_{dc} \simeq \frac{P^{RA}_{\rm intra}}{2\pi} \quad \text{(WDL)} \tag{47}$$

where the intraband term $P^{RA}_{\rm intra}$ coincides with the first term on the r.h.s. of Eq. (37). By using the result (46) for the anomalous vertex we can rewrite it as follows

$$P^{RA}_{\rm intra} = \frac{\left[p_+^2 + p_-^2\right]}{4m\Gamma} \qquad E_F > E_0 \tag{48}$$

$$P^{RA}_{\rm intra} = \frac{\left[p_+^2 - p_-^2 - m\tilde{\alpha}_{RA}(p_+ - p_-)\right]}{4m\Gamma} \qquad E_F < E_0. \tag{49}$$

Using the expression of $p_\pm$, Γ and $\tilde{\alpha}^{RA}$ derived above, along with the expressions for the particle density in the WDL, i.e.

$$n = \begin{cases} (m/\pi)(E_F + E_0) & E_F > E_0 \\ (p_0^2/\pi)\sqrt{E_F/E_0} = n_0\sqrt{E_F/E_0} & E_F < E_0 \end{cases} \tag{50}$$

Eq.s (48-49) lead to the final expression for the conductivity quoted in Eq.s (1)-(2) of the main text.

To conclude this section we would like to show that the inclusion of vertex corrections is crucial in both regimes. The "bare-bubble" conductivity σ_{bb}, corresponding to the first diagram in Fig. 6, is given by the term P_0 defined in Eq. (36). It can be directly computed from Eq. (37) by replacing $\tilde{\alpha}$ with α, so that the renormalized velocity $\vec{V}_{\mathbf{p}s}$ is replaced by the bare one $\vec{v}_{\mathbf{p}s}$. In the WDL we then easily obtain

$$P^{RA}_{bb} = \frac{\pi}{2\Gamma\mathcal{V}}\sum_{\mathbf{p},s}\vec{v}^2_{\mathbf{p}s}\delta(E^s_{\mathbf{p}} - E_F) = \frac{v_F}{4\Gamma}(p_+ + p_-) \tag{51}$$

Thus, using Eq.s (43), (45) and (50) into Eq. (47) one easily obtains that (restoring the charge e)

$$\sigma_{\rm bb} = \frac{e^2(n - n_0/2)}{2m\Gamma} = \sigma_{\rm Drude} - \sigma_{n_0}, \quad E_F > E_0 \tag{52}$$

$$\sigma_{\rm bb} = \frac{e^2 n}{4m\Gamma} = \frac{\sigma^{WDL}_{\rm Drude}}{2}, \qquad E_F > E_0 \tag{53}$$

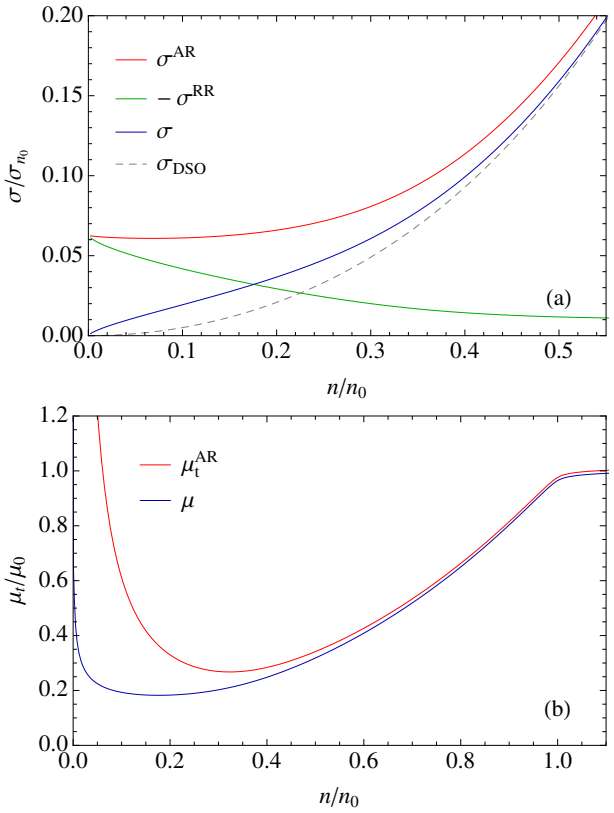

Figure 8: (Color online) (a) Different contributions to the conductivity as a function of the density for $E_0 = 40\Gamma_0$, $\Gamma_0 = 0.5meV$ and $m = 0.7m_e$. (b) Comparison of the total the AR mobilities. Parameters as in panel (a).

where, as in the main text, $\sigma_{\rm Drude} = e^2 n/(2\Gamma_0 m)$, $\sigma_{n_0} = e^2 n_0/(4\Gamma_0 m)$ and $\sigma^{WDL}_{\rm Drude} = e^2 n/(2\Gamma^{WDL} m)$. We therefore see that the bare-bubble result is inadequate at all densities and chemical potentials. This also shows that even recovering the Drude conductivity at $E_F > E_0$ is a non-trivial result, due to the crucial role of vertex corrections. Indeed, even in the regime $E_F \gtrsim E_0$, where E_F slightly exceeds the Rashba energy, so that two Fermi surfaces are clearly separated, any signature of the Rashba interaction disappears in the dc conductivity, which is given by the usual Drude formula. We also notice that vertex corrections tend to enhance the conductivity with respect to the bare-bubble result. As we shall discuss below, this is the result one usually expects within a Boltzmann picture, where backward and forward scattering processes contribute to the transport scattering time with different weights.

Relevance of the RR contribution

As we mentioned above, our analytical formulae are in principle valid only in the WDL, realized for $\Gamma \ll E_F$. In

this limit we did two approximations, we replaced the spectral functions of the chiral eigenstates with delta functions and neglected the RR part in Eq. (26). As the density decreases in the DSO regime these approximations are not valid anymore and the quantum result for σ_{dc} starts to deviates from the analytical WDL result σ_{DSO}. In this regime the RR current response function becomes as much relevant as the RA one, and it is important to include it in order to reproduce physical results for the dc conductivity. In Figure 8(a) we plot separately the contributions of the RR and AR response function to the conductivity, defined respectively as $\sigma^{AR} = P^{AR}(0,0)/(2\pi)$ and $\sigma^{RR} = -P^{RR}(0,0)/(2\pi)$. As one can see, for our parameters choice, at $n/n_0 \lesssim 0.5$ the RR contribution increases, while the AR one tends to saturates with decreasing density. Neglecting σ_{RR} thus leads to the unphysical result of a finite conductivity for zero density. The vanishing of the conductivity as $n \to 0$ is indeed guaranteed by the cancellation between σ^{AR} and σ^{RR}. This fact is also evident in Fig. 8(b) where along with the total mobility μ_t we also plot the "AR" mobility, μ_t^{AR} defined as $\mu_t^{AR} = \sigma^{AR}/n$. We se that the inclusion of the RR contribution significantly modifies the structure of the mobility curves around the minimum. Eventually we note that the cancellation between RR and AR terms turns out to improve the agreement between σ_{dc} and σ_{DSO} and it enlarges the range where the DSO formula can be used to describe transport.

DC CONDUCTIVITY WITHIN SEMICLASSICAL BOLTZMANN APPROACH

For a detailed discussion of Boltzmann equation we refer the reader to Ref.[4], here we only outline the most significant steps. Note that here we neglect the effect of the off-diagonal terms of the spin-density matrix in the helicity basis at a given $\mathbf{p}$ since as discussed in the main text they give only small corrections to dc charge transport (see e.g. Refs.[5, 6, 9, 10]). Let us call $\rho_{\mathbf{p},s}$ the distribution function for the quasiparticle eigenstates $\varepsilon_{\mathbf{p},s}$, where s denotes in general the band index, which coincides in our case with the chiral index. The time derivative of ρ is determined by the collision integral:

$$\frac{\partial \rho_{\mathbf{p},s}}{\partial t} = -\sum_{\mathbf{p}',s'} Q^{\mathbf{p}s}_{\mathbf{p}'s'}[\rho_{\mathbf{p},s} - \rho_{\mathbf{p}',s'}], \tag{54}$$

where $Q^{\mathbf{p}s}_{\mathbf{p}'s'}$ is the scattering kernel from the state $\varepsilon_{\mathbf{p},s}$ to the state $\varepsilon_{\mathbf{p}',s'}$. In the presence of an electric field $\mathbf{E}$ the l.h.s. of the above equations is given by:

$$\frac{\partial \rho_{\mathbf{p},s}}{\partial t} = -e\mathbf{E}\cdot\frac{\partial \rho_{\mathbf{p},s}}{\partial \mathbf{p}} \simeq -e\mathbf{E}\cdot\vec{v}_{\mathbf{p}s}\frac{\partial \rho^{\rm eq}_{\mathbf{p},s}}{\partial \varepsilon_{\mathbf{p}s}} \tag{55}$$

in the last passage we replaced ρ with its equilibrium value $\rho^{\rm eq}_{\mathbf{p},s} \equiv f(\varepsilon_{\mathbf{p}s})$, since we are interested in the linear response in $\mathbf{E}$. In the relaxation-time approximation we can express the time evolution of ρ via a transport scattering time τ^{tr}_{ps}, so that:

$$\frac{\partial \rho_{\mathbf{p},s}}{\partial t} = -\frac{\rho_{\mathbf{p},s} - \rho^{\rm eq}_{\mathbf{p},s}}{\tau^{tr}_{ps}} \tag{56}$$

By combining Eqs. (55)-(56) we then have:

$$\rho_{\mathbf{p},s} = \rho^{\rm eq}_{\mathbf{p},s} + e\mathbf{E}\cdot\vec{v}_{\mathbf{p}s}\tau^{tr}_{ps}\frac{\partial \rho^{\rm eq}_{\mathbf{p},s}}{\partial \varepsilon_{\mathbf{p}s}}. \tag{57}$$

For a field in the x direction the current can then be written as:

$$j_x = -e\sum_{\mathbf{p}s} v^x_{\mathbf{p}s}\rho_{\mathbf{p},s} = e^2E_x\sum_{\mathbf{p}s}(v^x_{\mathbf{p}s})^2\tau^{tr}_{ps}\left(-\frac{\partial \rho^{\rm eq}_{\mathbf{p},s}}{\partial \varepsilon_{\mathbf{p}s}}\right) \tag{58}$$

where we used the fact that there is no current in the equilibrium state. At $T = 0$ we can put $\partial\rho^{\rm eq}_{\mathbf{p},s}/\partial\varepsilon_{\mathbf{p}s} = \partial f(\varepsilon_{\mathbf{p}s})/\partial\varepsilon_{\mathbf{p}s} = \delta(\varepsilon_{\mathbf{p}s}-\mu)$. Thus, by identifying $\varepsilon_{\mathbf{p}s}-\mu \equiv E^s_{\mathbf{p}} - E_F$ we arrive at Eq.(8) of the main text

$$\sigma_{dc} = \frac{e^2}{2}\sum_{\mathbf{p}s}|\vec{v}_{\mathbf{p}s}|^2\tau^{tr}_{ps}\delta(E_{\mathbf{p}s} - E_F) \tag{59}$$

A set of equations for the transport scattering times can be derived by substitution of Eq. (55) into Eq. (54), once that one uses the *Ansatz* (56). By doing so, since the scattering kernel Q conserves the energy, and the equilibrium function $\rho^{\rm eq}_{\mathbf{p},s}$ does not depend on the chiral index but only on the energy, one is left with:

$$\begin{aligned}\vec{v}_{\mathbf{p}s} &= \sum_{\mathbf{p}'s'} Q^{\mathbf{p}s}_{\mathbf{p}'s'}\left[\tau^{tr}_{ps}\vec{v}_{\mathbf{p}s} - \tau^{tr}_{p's'}\vec{v}_{\mathbf{p}'s'}\right] = \\ &= \frac{\tau^{tr}_{ps}}{\tau\left(E^s_p\right)}\vec{v}_{\mathbf{p}s} - \sum_{\mathbf{p}'s'} Q^{\mathbf{p}s}_{\mathbf{p}'s'}\tau^{tr}_{p's'}\vec{v}_{\mathbf{p}'s'},\end{aligned} \tag{60}$$

where we introduced the quasiparticle scattering time

$$\frac{1}{\tau\left(E^s_p\right)} = \sum_{\mathbf{p}'s'} Q^{\mathbf{p}s}_{\mathbf{p}'s'}. \tag{61}$$

By using the fact that only the component of $\vec{v}_{\mathbf{p}'s'}$ in the direction of $\vec{v}_{\mathbf{p}s}$ survives after momentum integration, Eq. (60) finally reduces to Eq.(9) of the main text

$$\frac{\tau^{tr}_{ps}}{\tau\left(E^s_p\right)} = 1 + \sum_{\mathbf{p}'s'} Q^{\mathbf{p}s}_{\mathbf{p}'s'}\tau^{tr}_{p's'}\frac{\vec{v}_{\mathbf{p}'s'}\cdot\hat{v}_{\mathbf{p}s}}{|\vec{v}_{\mathbf{p}s}|} \tag{62}$$

Notice that Eq. (62) differs from the one proposed *e.g.* in Ref. [7], where the band-dependence of the transport scattering times on the r.h.s. of Eq. (62) has been overlooked, leading to decoupled equations for the τ^{tr}_{ps}. Here instead the set of coupled equations (62) is analogous to the self-consistence equations (29) introduced above for the renormalized current in the quantum language. This

analogy can be exploited further by the identification of the renormalized Boltzmann current as

$$\mathbf{J}^B_{\mathbf{p}s} = e\vec{v}_{\mathbf{p}s}\frac{\tau^{tr}_{ps}}{\tau\left(E^s_p\right)} \tag{63}$$

As already discussed in Ref. [8] for the case $E_F > E_0$, both the quantum and the Boltzmann approaches lead to the same renormalized currents. This result also holds in the DSO regime $E_F < E_0$, as one can see from the explicit solution for the τ's derived below.

Collision integral

By using Fermi Golden Rule, the scattering rate from the state $|\mathbf{p}, s\rangle$ to the state $|\mathbf{p}', s\rangle$ can be written as:

$$Q^{\mathbf{p}s}_{\mathbf{p}'s'} = \frac{2\pi}{V}|\langle \mathbf{p}s|V_{\rm imp}|\mathbf{p}'s'\rangle|^2\delta(\varepsilon_{\mathbf{p}s} - \varepsilon_{\mathbf{p}'s'}) \tag{64}$$

Using the explicit expression of the helicity eigenstates in plane waves, we can rewrite the above equation as follows:

$$Q^{\mathbf{p}s}_{\mathbf{p}'s'} = \frac{2\pi}{\mathcal{V}^2}\left|\int d\mathbf{r}\, e^{i(\mathbf{p}-\mathbf{p}')\mathbf{r}}V_{\rm imp}(\mathbf{r})W^{\mathbf{p}\mathbf{p}'}_{s's}\right|^2\delta(E^s_{\mathbf{p}} - E^{s'}_{\mathbf{p}'}) \tag{65}$$

Here the matrix $\hat{W}^{\mathbf{p}\mathbf{p}'} = U^\dagger_{\mathbf{p}'}U_{\mathbf{p}}$ comes from the scalar product of the helicity eigenvectors. Within our approximations, (self-averaging delta-correlated disorder and Born scattering), we can write $\langle V_{\rm imp}(\mathbf{r})V_{\rm imp}(\mathbf{r}')\rangle \simeq n_i v^2_{\rm imp}\delta(\mathbf{r}-\mathbf{r}')$ and we can recast the above equation as

$$Q^{\mathbf{p}s}_{\mathbf{p}'s'} = \frac{2\pi}{\mathcal{V}}n_i v^2_{\rm imp}\left|W^{\mathbf{p}\mathbf{p}'}_{s's}\right|^2\delta(E^s_{\mathbf{p}} - E^{s'}_{\mathbf{p}'}). \tag{66}$$

where

$$|W^{\mathbf{p}\mathbf{p}'}_{s's}|^2 = \frac{1+{\rm sign}(ss')\cos(\theta_{\mathbf{p}}-\theta_{\mathbf{p}'})}{2},$$

so that one recovers Eq. (5) of the main text.

Solution of Boltzmann equations

Using the explicit expression of $Q^{\mathbf{p}'s'}_{\mathbf{p}s}$, Eq.(62) reads

$$\frac{\tau^{tr}_{ps}}{\tau\left(E^s_p\right)} = 1 + \frac{\pi n_i v^2_{\rm imp}}{\mathcal{V}}\sum_{\mathbf{p}'s'}(1+ss'\hat{p}\cdot\hat{p}')\frac{\vec{v}_{\mathbf{p}'s'}\cdot\hat{v}_{\mathbf{p}s}}{|\vec{v}_{\mathbf{p}s}|}\cdot \cdot\delta(E^s_{\mathbf{p}} - E^{s'}_{\mathbf{p}'})\tau^{tr}_{p's'}. \tag{67}$$

Now recalling that $\vec{v}_{\mathbf{p}s} = v_{\mathbf{p}s}\hat{p}$ and that $|\vec{v}_{\mathbf{p}s}| = v_F = \sqrt{2mE_F}$ for $E^s_{\mathbf{p}} = E_F$, for states at the Fermi level we can rewrite the above equation as:

$$\frac{\tau^{tr}_{ps}}{\tau} = 1 + \frac{\pi n_i v^2_{\rm imp}}{\mathcal{V}}\sum_{\mathbf{p}'s'}(\hat{p}\cdot\hat{p}')^2\eta_{ps}\eta_{p's'}\delta(E_F - E^{s'}_{\mathbf{p}'})\tau^{tr}_{p's'} \tag{68}$$

where we set $\tau(E_F) = \tau$ and $\eta_{ps} = s(\hat{v}_{\mathbf{p}s}\cdot\hat{p}) = \pm 1$. Performing the angular integral $\mathbf{p}'$ and changing variables from p, s to E, η we eventually recover equation (10) of the main text:

$$\frac{\tau^{\rm tr}_\eta}{\tau} = 1 + \frac{1}{4\tau_0 m v_F}\sum_{\eta'}\eta\eta' p_{\eta'}\tau^{\rm tr}_{\eta'}, \tag{69}$$

where τ_0 denotes as usual the quasiparticle scattering time in the absence of spin-orbit, $\tau_0 = 1/(mn_i v^2_{\rm imp})$, $p_\eta = p_\eta(E_F)$ indicate the two Fermi momenta introduced in Eqs.(43) and we set $\tau^{\rm tr}_\eta = \tau^{\rm tr}_\eta(E_F)$.

To solve this equation it is useful to note that $\tau/\tau_0 = mv_F/\bar{p}_F$ where $\bar{p}_F = 1/2\sum_\eta p_\eta$ that allows us to recast Eq. 69 as:

$$\bar{\tau}^{\rm tr}_\eta = 1 + \frac{1}{4}\sum_{\eta'}\eta\eta'\bar{p}'_\eta\bar{\tau}^{\rm tr}_{\eta'}. \tag{70}$$

with $\bar{\tau}^{\rm tr}_\eta = \tau^{\rm tr}_\eta/\tau$ and $\bar{p}_\eta = p_\eta/\bar{p}_F$. As one can easily check, the solution of this equation reads: $\bar{\tau}^{\rm tr}_\eta = \bar{p}_\eta$ that coincides with Eq. (12) of the main text.

[1] G. D. Mahan, *Many-Particle Physics* (Springer, Berlin-Heidelberg, 2000).
[2] H. Bruus and C. Flenshberg, *Many-Body Quantum Theory in Condensed Matter Physics* (Oxford University Press, New York, 2004).
[3] A. Knigavko and J. P. Carbotte Phys. Rev. B 72, 035125 (2005).
[4] J. M. Ziman, *Principles of the Theory of Solids* (Cambridge University Press, Cambridge, United Kingdom, 1972).
[5] M. I. Dyakonov and A. V. Khaetskii, Zh. Eksp. Teor. Fiz. **86**, 1843 (1984).
[6] A. V. Khaetskii, Phys. Rev. Lett. **96**, 056602 (2006).
[7] N. A. Sinitsyn, A. H. MacDonald, T. Jungwirth, V. K. Dugaev, and Jairo Sinova, Phys. Rev. B 75, 045315 (2007)
[8] P. Schwab and R. Raimondi, Eur. Phys. J. B **25**, 483 (2002).
[9] A. V. Shytov, E. G. Mishchenko, H.-A. Engel, and B. I. Halperin Phys. Rev. B **73**, 075316 (2006).
[10] R. Raimondi, C. Gorini P.Schwab M. Dzierzawa, Phys. Rev B **74**, 035340 (2006).